stabilize the CDW-Mott phase in terms of band engineering. The discovery of the robust CDW-Mott phase far above room temperature is considered valuable for developing practical CDW-Mott insulator-based ultrathin nanoelectronic devices. (Reported by Ashish Chainani)

This report features the work of Takafumi Sato, Katsuaki Sugawara and their collaborators published in Nat. Commun. ***12****, 5873 (2021).*

TLS 21B1 Angle-resolved UPS

- ARPES
- Materials Science, Condensed-matter Physics

References

1. P. Fazekas, E. Tosatti, Philos. Mag. B **39**, 229 (1979).
2. K. Rossnagel, N. V. Smith, Phys. Rev. B **73**, 073106 (2006).
3. K. S. Novoselov, D. Jiang, F. Schedin, T. J. Booth, V. V. Khotkevich, S. V. Morozov, A. K. Geim. PNAS **102**, 10451 (2005).
4. Y. Nakata, K. Sugawara, A. Chainani, H. Oka, C. Bao, S. Zhou, P.-Y. Chuang, C.-M. Cheng, T. Kawakami, Y. Saruta, T. Fukumura, S. Zhou, T. Takahashi, T. Sato, Nat. Commun. **12**, 5873 (2021).

A Route to Create Quantum Spin Hall Systems

A novel phenomenon termed the topological proximity effect, which occurs between a 2D material and a 3D topological insulator, has generated a paradigm that opens a route to create quantum spin Hall systems in monolayer-substrate heterostructures.

3D topological insulators (TI), which refer to the states of matter with an insulating gap in the bulk and gapless helical states on the surface, have attracted much attention due to their fascinating electronic structures. Proximity effects that occur in heterojunctions comprised of TIs and materials can provide an interesting platform to produce emerging quantum phenomena of Dirac fermions at the interfaces. For instance, it has been predicted that a hybrid structure made of a 3D TI and a superconductor can produce a superconducting proximity effect at the interface, which might lead to the emergence of 2D topological superconductivity hosting Majorana fermions. In graphene transferred on 3D TI, a strong proximity effect can induce opening of the band gap and strong spin-orbital coupling, which leads to a strong tunability and suppression of the spin signal and lifetime. Moreover, the predictions of such an interaction with non-topological states at the interface between a normal insulator (NT) and a TI might result in vertical twinning of the Dirac cone; the non-topological states can acquire a spin texture without magnetic doping. The study of the band structure of 2D NI/3D TI is significant to understand topological proximity effect; the results bear great potential for spintronics.

Herein, Jung-Chun Andrew Huang (National Cheng Kung University), Tay-Rong Chang (National Cheng Kung University), Cheng-Maw Cheng (NSRRC) and their teams studied a novel phenomenon termed a topological proximity effect, which occurs between a 2D material and a 3D TI. To understand further the change of electronic structure between Sb_2Te_3 and the antimonene/Sb_2Te_3 hybrid heterostructure, they performed an experiment at **TLS 21B1** beamline of the Taiwan Light Source recording angle-resolved photoemission spectra (ARPES) to probe the band structures. **Figures 1(a) and 1(b)** (see next page) show the band-mapping results of pristine Sb_2Te_3 and antimonene/Sb_2Te_3 recorded along the Γ-K direction. In a comparison of the two band-mapping results along direction Γ-K between Sb_2Te_3 and antimonene/Sb_2Te_3, an additional Sb-bilayer (BL)-derived band is observed near the Fermi level; the band structure of Sb_2Te_3 has a rigid band shift to larger binding energy. **Figure 1(c)** shows an enlargement of the energy scale in **Fig. 1(b)** to resolve the band dispersion around the Fermi level. The two Sb-BL-derived bands have an intersection at the Γ point near the Fermi level; a new Dirac point D_{sb} is located almost at the Fermi level. The observed band dispersion indicates that a new topological state has been formed in the antimonene/Sb_2Te_3 hybrid-heterostructure.

Figure 1(d) shows the calculated surface spectral weight with a color corresponding to the integrated charge

density of the state within the Sb-BL, topmost quintuple layer (QL) (first QL), and the nearest-neighboring QL (second QL) in Sb_2Te_3. **Figures 1(e) and 1(f)** display the wide range and a magnification of the calculated band structures superimposed on the ARPES band mapping, respectively. The density-functional theory (DFT) calculations identify that the linear Dirac state near E_F is derived from the Sb-BL. The free-standing Sb-BL is notably predicted to be a NI with band gap 2.28 eV. The topological Dirac state can thus be expected to appear at the interface between NI Sb-BL and TI Sb_2Te_3 in the Sb-BL/Sb_2Te_3 hybrid structure based on a concept of a bulk-boundary correspondence. Surprisingly, their calculations manifest that the topological Dirac state is contributed mainly from the Sb-BL, whereas the band dispersion of the first QL and second QL in Sb_2Te_3 presents an energy gap. Following the idea of topological band theory, the covered Sb-BL can be effectively regarded as a new surface of the Sb-BL/Sb_2Te_3 hybrid structure. Sb-BL is hence topologicalized because of the proximity effect between Sb-BL and Sb_2Te_3. The interaction between the adjacent NI and TI is complicated. One possibility comes from the energy band hybridization between NI and TI because the type-II band alignment at the interface between NI and TI, that is, the valence-band maximum of a NI, is in the band gap of the TI, which might lead to an anti-crossing between the valence state of NI and the Dirac surface state of the TI, resulting in a new surface state that exists in the adjacent NI. The position of the Dirac point and the shape of the Dirac surface state can consequently be tuned on varying the energy position of the valence band of the NI, for example on altering the doping level. This advantage might be used to manipulate the topological properties of 2D materials. More importantly, the spin spectral weights in the Sb-BL near the Fermi level exhibit clear spin-polarized states. In addition to the topological surface state, a quasi-linear spin-polarized band was found above E_F in the first QL. Interestingly, the chirality of its spin texture is opposite that of the Dirac state of Sb-BL. Contrary to the spin-momentum locked spin texture in plane, an additional S_z spin band out of plane appears below E_F in Sb-BL and the first QL, which is likely due to the strong warping effect in the hexagonal lattice. As a result, the direction of the spin texture of Sb-BL/Sb_2Te_3 becomes greatly modified *via* varying the Fermi level. Through the proximity effect induced at the interface, the antimonene/Sb_2Te_3 2D NI/3D TI system provides a promising way to form a new TI state and to tune the position of the Dirac point.

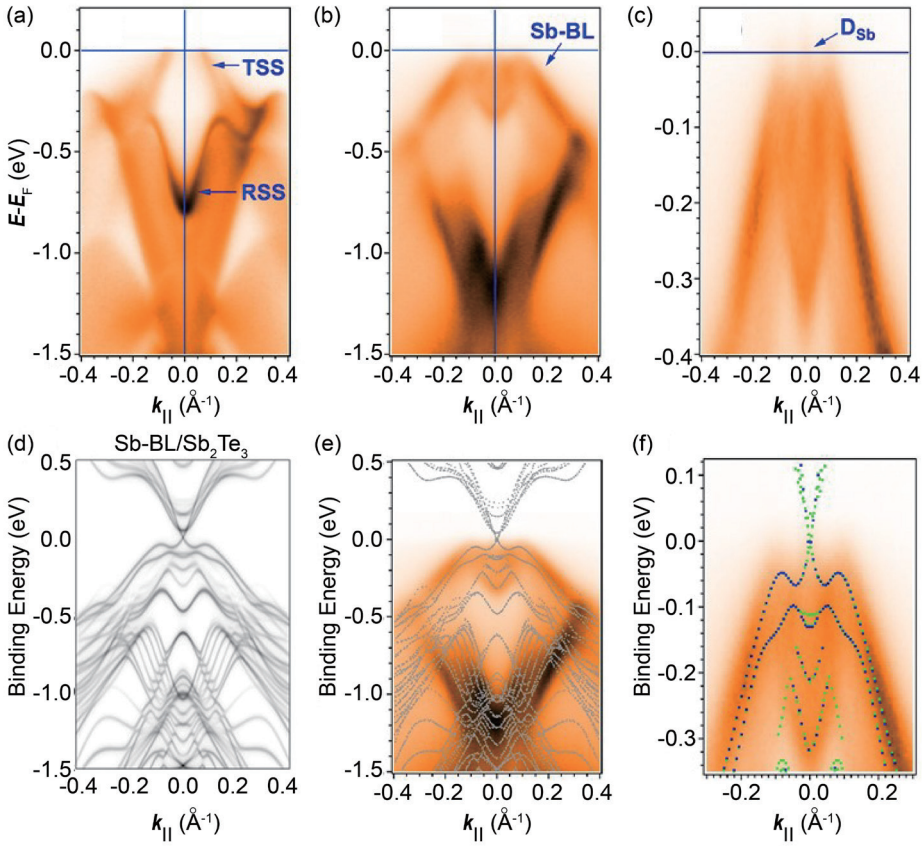

Fig. 1: (a) Band-mapping result of Sb_2Te_3 taken at photon energy 24 eV. (b) Band-mapping result of antimonene/Sb_2Te_3 taken at photon energy 24 eV. (c) Enlarged energy scale of the band-mapping result in (b). (d) Calculated band structure of Sb-BL/Sb_2Te_3. (e) Overlapping band dispersion extracted from (d) on the band-mapping result of antimonene/Sb_2Te_3. (f) Enlargement of energy and momentum scales in (b). [Reproduced from Ref. 1]

In summary, the authors provide strong evidence derived from hydrogen etching on Sb_2Te_3 that large-area and well ordered antimonene presents a 2D topological state. A new topological state formed in the antimonene/Sb_2Te_3 heterostructure was confirmed with ARPES and calculations with DFT; in particular, the Dirac point was located almost at the Fermi level. The results reveal that Dirac fermions are indeed realized at the interface of a 2D NI and a 3D TI as a result of strong hybridization between antimonene and Sb_2Te_3. Due to the proximity effect induced at the interface, their work demonstrates that the antimonene/Sb_2Te_3 2D NI/3D TI system could provide a promising way to form a new TI state and to modify the direction of the spin texture of Sb-BL/Sb_2Te_3 *via* varying the Fermi level. (Reported by Cheng-Maw Cheng)

This report features the work of Jung-Chun Andrew Huang

*and Cheng-Maw Cheng and their collaborators published in ACS Nano **15**, 15085 (2021).*

TLS 21B1 Angle-resolved UPS

- ARPES
- Materials Science, Condensed-matter Physics

Reference

1. S. H. Su, P.-Y. Chuang, H.-Y. Chen, S.-C. Weng, W.-C. Chen, K.-D. Tsuei, C.-K. Lee, S.-H. Yu, M. M.-C. Chou, L.-W. Tu, H.-T. Jeng, C.-M. Tu, C.-W. Luo, C.-M. Cheng, T.-R. Chang, J.-C. A. Huang, ACS Nano **15**, 15085 (2021).

A Hallmark of Hund's Physics in the Multi-Orbital System

An abrupt deviation from Fermi liquid behavior has been directly observed in electron self-energy results as the kink feature at a low-energy scale. The results of the evolution of the characteristic temperature scale via a kink features, which is a hallmark of Hund's physics in a multi-orbital system.

Since Mott's initial proposal that an insulating ground state can appear due to the electron–electron correlation, the metal-insulator transition (MIT) has been at the core of condensed-matter physics. The Coulomb interaction U is the most important parameter; thus finding how the spectral function and energy scale evolve as a function of U has been a fundamental issue in MIT studies. The Brinkman-Rice picture and dynamical mean-field theory (DMFT) for the half-filled one-band Hubbard model show that the overall quasi-particle (QP) peak and Kondo temperature T_K gradually become renormalized as U increases. At the MIT, the QP mass diverges with vanishing T_K. Most realistic materials are, however, multi-orbital systems in which not only U but also Hund's coupling J_H is a critical parameter for the ground state. During the past decade, there has been a remarkable progress in the theoretical description of Hund's physics in correlated electron systems. It was found that J_H can enhance the effective correlation strength of multi-orbital systems by weakening the Kondo screening channel. The most drastic effect occurs in non-singly-occupied and non-half-filled cases such as iron pnictides, chalcogenides and ruthenates. Although these materials are metallic and are located far from the Mott insulating state, their small coherence energy scale due to J_H induces incoherent transport properties. These new phases are classified as Hund's metal; their correlated electronic structures have been intensively studied through both experimental and theoretical approaches.

An important remaining question is how J_H affects the evolution of the spectral function and the energy scale of multiband systems. Considering these aspects, $NiS_{2-x}Se_x$, a half-filled system with degenerate Ni e_g orbitals, is probably the most suitable multi-orbital system for an investigation of the evolution in the presence of J_H. On varying the Se content, the correlation strength can be easily tuned in the existence of J_H. To address the role of J_H during the MIT, Changyoung Kim (Seoul National University, Korea), Cheng-Maw Cheng (NSRRC) and their teams reexamined the band structure of $NiS_{2-x}Se_x$ not only with angle-resolved photoemission spectra (ARPES) with finer doping steps and higher resolution but also *via* density-functional theory (DFT) plus DMFT with and without J_H. They utilized ARPES to achieve the high resolution needed to observe clearly the QP of $NiS_{2-x}Se_x$. Their results reveal clear QP dispersions as well as doping-dependent low-energy kink structures. The DFT+DMFT calculations also identify the kink structures, which explain the strongly suppressed temperature scale due to J_H. The evolution of a kink observed in their ARPES data provides direct spectroscopic evidence for the evolution of the energy scale in the presence of J_H.

The α hole pocket is the most representative QP band for the Mott transition in $NiS_{2-x}Se_x$. As the Fermi-surface volume of the α band is much larger than the others, the transport properties of $NiS_{2-x}Se_x$ should be dominated by the hole pocket. To study how the α band dispersion varies across the MIT, they performed ARPES experiments at **TLS 21B1** beamline of the NSRRC. ARPES spectra along the Γ-X line were recorded at 16 K for diverse Se doping shown in **Fig. 1**. A QP band, distinct from the incoherent band (**Fig. 1(g)**), is clearly observed in all metallic samples, whereas the QP was not clearly discernible as it was buried under an incoherent spectral weight in previous reports (grey filled curve in **Fig. 1(g)**). The appearance or disappearance of the QP follows the MIT behavior along the Se doping; the QP is seen for the metallic phase ($x \geq 0.43$) whereas it is absent in the insulating phase ($x = 0.3$) (see **Fig. 1(a)** for the phase diagram).